ENGINEERING TRANSACTIONS • *Engng. Trans.* • **47**, 3–4, 321–337, 1999
Polish Academy of Sciences • Institute of Fundamental Technological Research
10.24423/engtrans.635.1999

MODELLING OF HOT METAL FORMING IN THE CONDITIONS OF VARIABLE STRAIN RATES AND TEMPERATURES

M. PIETRZYK

UNIVERSITY OF MINING AND METALLURGY KRAKÓW
Al. Mickiewicza 30, 30–059 Kraków

The model, based on the internal variable theory, describing behaviour of metals during hot plastic deformation, is presented. This model is coupled with a typical thermal-mechanical finite-element solution for hot metal forming processes. Problems connected with simulation of hot forming of steel and aluminium alloys in the variable conditions are discussed. Two types of materials are considered: i) those showing a delay of the response in transient conditions, ii) those reaching without delay a new level determined by the equation of state for new conditions of deformation. The model is verified experimentally.

1. INTRODUCTION

Understanding of basic principles of metal behaviour during plastic deformation is necessary for proper design of metal forming processes. Modelling of various phenomena, which take place during hot plastic deformation, is an important factor aiding the technology design. It enables the prediction of microstructure and properties of final product, which are often difficult to be determined experimentally [1, 2]. Several models describing the processes taking place during hot and cold plastic deformation, creep, superplastic deformation, annealing and fracture, have been elaborated. One should realise that most of these models do not have physical interpretation and further research should be carried out to improve them. These models usually fail in the case of processes characterised by variable conditions of deformation or varying directions of strains. Application of internal variables to the description of the state of material during hot deformation introduces a physical basis to the models.

Changes of the main directions of strains during plastic deformation are important both for the users of products (fatigue) and for the producers (e.g.

rolling). Even in the geometrically simple process like flat rolling, elements near the contact surface are subjected to a reverse shear strain. Figure 1 shows the calculated distributions of the longitudinal strain, the shear strain and the effective strain during rolling of a 20 mm thick plate with the reduction of 0.2. Calculations were performed using the program described in Sec.3. Reversed shear strains are well seen in Fig. 1. The shear strains have been calculated by integration of the shear strain rates along the flow lines in the roll gap. The integration leads to almost zero shear strains at the exit plane. Distribution of the longitudinal strain across the thickness at exit is uniform. Effective strains, which account for the contribution of the reversed shear strains, are distributed non-uniformly, with the lowest values in the centre of the plate.

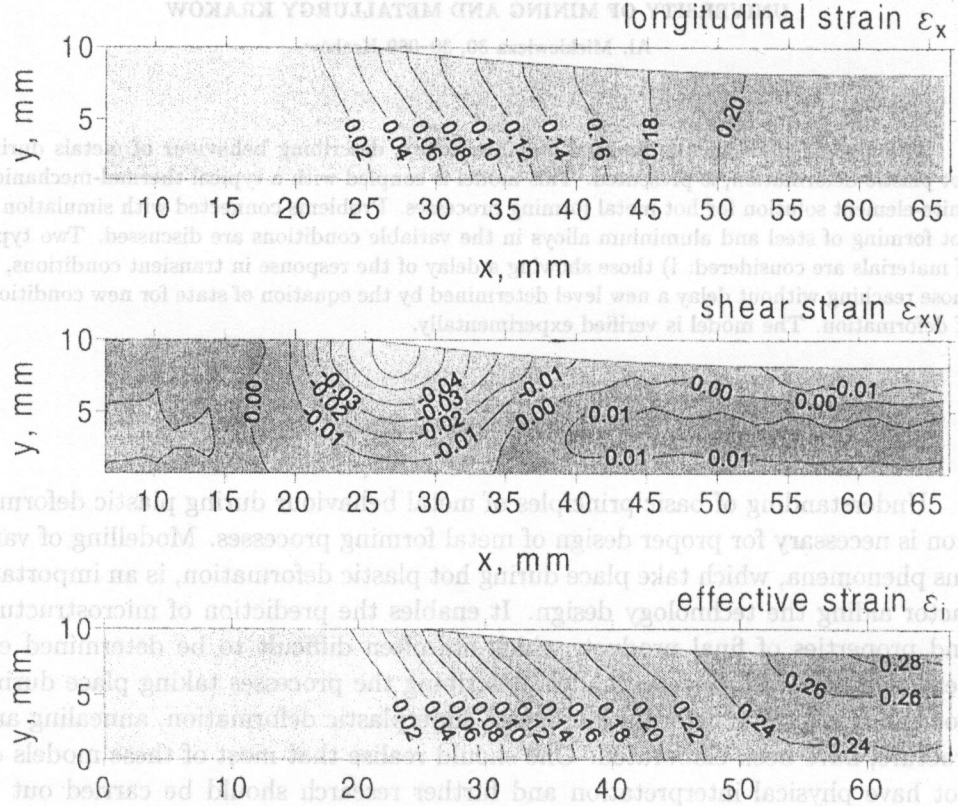

FIG. 1. Calculated distributions of the longitudinal strain, shear strain and effective strain during rolling of 20 mm thick plate, reduction 0.2. Due to symmetry, only upper half of the roll gap is presented.

Reversed shear strains are not so large in rolling; however, they may reach larger values in other forming processes. These strains may influence some mi-

crostructural parameters during hot deformation, such as kinetics of recrystallisation or grain size [3]. Reversed strains usually affect both the external variables (yield stress) and the internal variables (energy accumulated in the dislocation substructure). Several researchers showed that yield stress of various metals and alloys decreases when the strain is reversed [3] or when the main directions of strains are changed [4]. The objectives of the present work are formulated with the above remarks in mind. They include modelling of hot deformations in the variable conditions, including changes of strain rate or temperature or strain directions during the process. The model based on the internal variable approach achieves this objective.

2. Internal variable model

A general frame for the model is given on the basis of its application as a constitutive law, as described by Estrin [5]. He shows how the problem of constitutive modeling can be reduced to operating with a scalar instead of tensorial quantities. The components of the tensor of total strain rate $\dot{\varepsilon}$ are given by the sum of the elastic and plastic components, $\dot{\varepsilon}^e$ and $\dot{\varepsilon}^p$, respectively,

$$\dot{\varepsilon} = \dot{\varepsilon}^e + \dot{\varepsilon}^p. \tag{2.1}$$

The elastic part obeys the Hooke's law, while the plastic component of the strain rate tensor is expressed in the form of the Lévy-von Mises equation. In this equation the Huber-Mises effective quantities:

$$\dot{\varepsilon}_i^p = \sqrt{\frac{2}{3}\dot{\varepsilon}_{ij}^p \dot{\varepsilon}_{ij}^p} \qquad \text{(effective plastic strain rate)} \tag{2.2}$$

and

$$\sigma_i = \sqrt{\frac{3}{2}\sigma_{ij}\sigma_{ij}} \qquad \text{(effective stress)} \tag{2.3}$$

are used. This implies plastic isotropy of the material during deformation. The specifics of the model enter through the particular form of the equation relating the effective plastic strain rate and the effective stress referred to as *kinetic equation* (see Mecking and Kocks [6], Estrin and Mecking [7]). Material characteristics given by the experimental data, which are obtained in the plastometric tests, impose the choice of a suitable form of the kinetic equation operating with a scalar. A power-law is the most commonly used form of this equation:

$$\dot{\varepsilon}_i^p = \dot{\varepsilon}_0 \left(\frac{\sigma_i}{\sigma}\right)^n, \tag{2.4}$$

where σ – an internal variable representing the state of the material, $\dot{\varepsilon}_0, n$ – material parameters.

Equation (2.4) is just a convenient representation of the Arrhenius equation for thermally activated plastic flow by dislocation glide. Accordingly, the temperature dependence of the plastic strain rate is contained in the stress exponent n, which is a function of the activation volume for the underlying thermally activated dislocation mechanism, the Boltzmann constant and the absolute temperature. The parameter is proportional to the density of mobile dislocations. Another variant of the kinetic equation, in which the Arrhenius form is preserved, is:

$$\dot{\varepsilon}_i^p = \dot{\varepsilon}_0 \exp\left\{-\frac{\Delta G_0}{\sigma T}\left[1-\left(\frac{\sigma_i}{\sigma}\right)^p\right]^q\right\}, \tag{2.5}$$

where: ΔG_0 – the Gibbs free energy of activation at zero stress, σ – Boltzmann constant, p, q – material parameters determined from fitting the $\dot{\varepsilon}_i^p vs. \sigma_i$ curve, $\dot{\varepsilon}_0$ – constant.

It should be noted that in the limit of $\sigma_i \to 0$, Eq. (2.5) yields a finite plastic strain rate. In what follows, the kinetic equation in the form of Eq. (2.5) will be used. Thus, it should be implied that a definite non-zero plastic strain rate corresponds to any value of stress, however small it may be. It means that this model is characterized by no yielding and loading/unloading condition. A number of constitutive models [6, 7] share this property.

The kinetic equation refers to a fixed microstructure, i.e. to a constant value of the internal variable σ. However, as the microstructure varies in the process of hot plastic deformation, a separate equation is needed to describe the evolution of σ. It can be written in a general form:

$$\frac{d\sigma}{d\varepsilon_i^p} = f\left(\sigma, \dot{\varepsilon}_i^p, T\right). \tag{2.6}$$

This equation suggests that the rate of change of the internal variable is determined by its current value and no memory or path-dependent effects are included. Once the concrete form of the function f is specified, the constitutive formulation is complete. According to the earlier discussion, the quantity σ is the sole internal state variable, which represents the microstructural state of a material [7]. However, it can generally be expected that several internal structure variables, characterized by different rates of relaxation towards their steady state values, are needed to describe properly the mechanical response of a material. More sophisticated models with two and more internal variables can be invoked [5], however, they are not discussed in the present work.

2.1. Hardening and recovery

The general framework of the one-internal variable model is presented on the basis of the research of MECKING and KOCKS [6]. Their model, known in the

scientific literature as Kocks-Mecking model (K-M model), can be considered as a fundamental approach that has pointed the direction for later developments and more recent theories. It is based on the kinetic relationship in the form of Eq. (2.5), where the internal variable σ is related to the total dislocation density ρ:

$$\sigma = M_T \alpha G b \sqrt{\rho}, \tag{2.7}$$

where G – the shear modulus, b – the Burgers vector, M_T – the average Taylor factor, α – a constant.

The model implies that the strength of the material is determined by dislocation-dislocation interactions. All other sources of resistance to dislocation glide have been disregarded at this stage. Arguments justifying this choice of the internal variable and proving that Eq. (2.7) can be assumed to have general validity are given in [5]. The Taylor factor M_T accounts for the texture evolution and will not be considered here.

The evolution equation for the dislocation density ρ is derived accounting for the concurrent effects of storage and recovery:

$$\frac{d\rho}{d\varepsilon} = \frac{1}{bl} - k_2 \rho \qquad \text{or} \qquad \frac{d\rho}{dt} = \frac{\dot{\varepsilon}}{bl} - k_2 \rho \dot{\varepsilon}, \tag{2.8}$$

where the recovery coefficient is strain-rate and temperature-dependent:

$$k_2 = k_{20} \left[\frac{\dot{\varepsilon}}{\dot{\varepsilon}_0} \exp\left(-\frac{Q_s}{RT} \right) \right]^{1/n}. \tag{2.9}$$

In Eq. (2.9) k_{20} is a constant. The temperature dependence of k_2 at high temperatures is contained in the Arrhenius term in the Eq. (2.9), while n is a constant, typically about 4. In the low temperature range, the temperature dependence is contained in n, and then n is inversely proportional to T, while the Arrhenius term is omitted. In Eq. (2.9) Q_s represents the activation energy for dislocation climb equal to that for self-diffusion [7].

The recovery processes included in the equation (2.8) are of dynamic origin. Static recovery, in which a decrease of the dislocation density is proportional to the corresponding time increment, can be introduced in equation (2.8) in the following way:

$$\frac{d\rho}{dt} = \frac{\dot{\varepsilon}}{bl} - k_2 \rho \dot{\varepsilon} - R_\nu. \tag{2.10}$$

Assuming that static recovery is driven by the stress determined by the square root of the current dislocation density, a reasonable phenomenological model for the static recovery coefficient, R_ν, is [5]:

$$R_\nu = R_{\nu 0} \exp\left(-\frac{C_0}{\sigma T} \right) \sin h \left(\frac{C_1 \sqrt{\rho}}{\sigma T} \right), \tag{2.11}$$

where $R_{\nu 0}$, C_0 and C_1 are constants.

The form of the evolution Eq. (2.8) for the dislocation density provides a possibility of incorporating in the model metallurgical characteristics and microstructural features of the material. In a material, which is coarse-grained and single-phase, the only kinds of obstacles to moving dislocations will be those related to the dislocation structure itself and those provided by the grain boundaries. Regardless of how the dislocations are arranged, whether completely at random or in a cell or subgrain boundary structure, the mean free path of dislocations l is proportional to $\rho^{-0.5}$. Since the free path l is usually much smaller than the grain size of the material, Eq. (2.8) becomes:

$$\frac{d\rho}{dt} = k_1 \dot{\varepsilon} \sqrt{\rho} - k_2 \rho \dot{\varepsilon}, \tag{2.12}$$

where k_1 and k_2 are constants, with k_2 being given by Eq. (2.9).

The constitutive Eq. (2.12) can be integrated analytically, at least for the case of uniaxial deformation with constant plastic strain rate [6] and for constant stress creep [7]. The hardening term in Eq. (2.12) has to be changed when the density of geometrical obstacles becomes larger than that of the obstacles caused by other dislocations in the population. The mean free path l is then identified with spacing between these geometrical obstacles d. Assuming that the distance between obstacles does not change during the deformation and, further, that the obstacles do not affect the recovery coefficient k_2, their only influence on the flow stress will be through the effect on the rate of dislocation density. The kinetic equation is then still given by Eq. (2.4), whereas the evolution equation for dislocation density is written as:

$$\frac{d\rho}{dt} = \frac{\dot{\varepsilon}}{bd} - k_2 \rho \dot{\varepsilon}. \tag{2.13}$$

It should be mentioned here that some of the scientists (SANDSTROM and LAGNEBORG [8, 9], ROBERTS and AHLBLOM, [10]) adopt a recovery term derived from Friedel's treatment of the climb-controlled dislocation network. This approach is related to the probability of dislocations meeting and annihilating one another, which is proportional to ρ^2:

$$\frac{d\rho}{dt} = \frac{\dot{\varepsilon}}{bd} - 2\tau M \rho^2, \tag{2.14}$$

where M is dislocation mobility which, in a pure metal, is directly related to the self-diffusion coefficient, τ is dislocation line energy.

KOCKS and MECKING [6] have argued that Friedel's development is based on a model for static rather than dynamic recovery and some caution must be exercised when applying it. A particular case to which the model represented by

Eqs. (2.13) or (2.14) will be applied is that of grain boundary hardening. ESTRIN [5] points out, however, that the limit case of the grain size being the smallest characteristic length in the structure, applies only for the sub-micron grain sizes warranting that $d < 10\rho^{-0.5}$. The modified constitutive model now given by Eq. (2.13), enables simple integration.

The above considerations apply if geometrical obstacles outnumber the dislocation-structure related ones. In a more general case, when a superposition of the immobilizing effects of both types of obstacles is considered, the inverse obstacle spacing $1/l$ in Eq. (2.8) can be expressed as a linear combination of the inverse spacing of the two types of obstacles taken separately. The resulting evolution equation for dislocation density is [7]:

$$\frac{d\rho}{dt} = \dot{\varepsilon}\left(\frac{1}{bd} + k_1\sqrt{\rho}\right) - k_2\rho\dot{\varepsilon}. \tag{2.15}$$

ESTRIN [5] presents an integration of the constitutive model (2.15). He also shows other applications of the model based on the kinematic Eq. (2.5), e.g. to describe plastic deformation of other systems where the dislocation mean free path is constrained by microstructural elements, such as precipitates or second-phase particles. The methodology, which is described above, can be used to account for the particle effects on the deformation behavior. The constitutive model based on the kinetic Eq. (2.5) can be as well formulated for materials containing a dispersion of non-shareable second-phase particles, such as non-coherent precipitates or oxide or carbide dispersions.

2.2. Recrystallisation

The theory described in the previous section is suitable for modelling the situations, in which dislocation interactions result as an immediate response of the system, which is the dynamic recovery. In real processes this is not always the case. It is well known, and can be confirmed by experiments, that an excess of stored energy leads to the occurrence of recrystallisation.

In metals of high stacking fault energy, dynamic recovery takes place rapidly and a steady state of stress is reached. This is a result of a balance between work hardening and recovery. The steady state is characterised by a subgrain size, which in general depends on the Zener-Hollomon parameter Z. Deformation of materials with medium or low stacking fault energy is characterised by slow dynamic recovery. Thus, usually the dislocation density is allowed to increase to an appreciable level and it causes an onset of dynamic recrystallisation before the steady state is reached. It seems that the dynamic recrystallisation is a well-known phenomenon now and its major features have been outlined. Never-

theless, there still remain many unresolved problems (McQUEEN [11]). A survey of research on hot deformation of steels shows, however, that researchers remain convinced that generally the material softening is caused by dynamic recrystallisation and plastic instabilities become less likely or frequent as the temperature increases and/or the strain rate diminishes. Indeed, some scientists have reported different effects for other materials. WIERZBINSKI and KORBEL [12] observed that, in the sequence of structural changes during hot deformation of Cu-10Ni alloy, the shear bands play the most important role in mechanical performance, while dynamic recrystallisation is a secondary phenomenon. However, for the objective of modelling the thermomechanical processing of steels, it is assumed in this work that when the dislocation density achieves its critical value, the dynamic recrystallisation starts and becomes the dominant softening phenomenon. This critical value of the dislocation density corresponds to the critical strain ε_c. For a given stacking fault energy, the critical strain is a function of temperature, strain rate and austenite grain size.

Assumption of dynamic recrystallisation, in turn, implies a delay in the response of the system whilst the required excess of energy accumulates and can be mathematically simulated by the modification of Eq. (2.13). This modification involves a parameter, which accounts for the development of the dislocation population (stored energy) to a point at which widespread elimination of dislocations is observed. Thus, recrystallisation is a discrete process, which requires that some threshold of the stored energy is exceeded and which needs some time to be completed. Therefore, there can always be a situation in which neighboring regions in the material have different values of the internal variable. It seems that a proper approach to this problem requires an analysis of the distribution of the internal variable within some small volume of the material. This approach will be discussed in the following sections, while a simplified model assuming an average dislocation density is described first.

It is claimed (see DAVIES [13]) that dislocations can be treated *en masse* without loosing any of the detail, which determines the behavior of a material. While hardening and recovery in this approach are well described by Eq. (2.13), modeling of recrystallisation requires an introduction of the threshold for the dislocation density and it involves an additional term in Eq. (2.13):

$$\frac{d\rho}{dt} = \frac{\dot{\varepsilon}}{bd} - k_2\rho\dot{\varepsilon} - k_3(\rho - \rho_c). \tag{2.16}$$

It can be shown that Eq. (2.16) allows modelling of behaviour of materials characterised by typical flow stress curves, with maximum followed by steady state flow. This equation, however, fails in the case of multi-stage deformation or the deformation, which takes place in variable conditions.

2.3. Distribution function model

To simulate these complex microstructural phenomena, the dislocation density cannot be treated as an average value. Rather, the entire spectrum of the dislocation densities has to be considered. To make it possible, the distribution function $G(\rho, t)$, suggested by SANDSTROM and LAGNEBORG [8, 9] and defined as a volume fraction which has the dislocation density between ρ and $\rho + d\rho$, is introduced. As a consequence, the equation, which describes the evolution of the dislocation populations accounting for recrystallisation, is:

$$\frac{dG(\rho,t)}{dt} = \phi(\Delta\varepsilon) - g(\varepsilon) - \frac{\nu\gamma}{D} m\tau\rho G(\rho,t). \tag{2.17}$$

In Eq. (2.17), $\phi(\Delta\varepsilon)$ represents athermal storage (hardening), $\Delta\varepsilon$ is strain increment, $g(\varepsilon)$ is thermally activated softening (recovery) and $\tau = \mu b^2/2$. This equation is discretised and solved, for each interval of dislocation density, together with equations describing the kinetics of recrystallisation and grain growth (see Table 1). The fraction of migrating grain boundary γ in Eq. (2.17) is controlled by the nucleation rate at the beginning of the recrystallisation and by grain impingement at the final stage. This leads to an assumption that γ is qualitatively controlled by the term $X(1 - X)$. PIETRZYK *et al.* [14] and PIETRZYK and KUZIAK [15] propose equations, which describe mobile fraction of the grain boundary γ (see Table 2).

Table 1. Cycles of the simulation performed at each time step of the finite-element solution

no.	process	variables	direction	condition	Ref.	equation
1	hardening	$\Delta\rho, \rho$	$\underleftarrow{\rho}$	$\dot{\varepsilon} > 0$	SANDSTROM and LAGNEBORG [8, 9]	$\frac{d\rho}{dt} = \frac{\dot{\varepsilon}}{bl}$
2	recovery	$\Delta\rho, \rho$	$\underrightarrow{\rho}$	always	SANDSTROM and LAGNEBORG [8, 9]	$\frac{d\rho}{dt} = -2M\tau\rho^2$
					ESTRIN and MECKING [7]	$\frac{d\rho}{d\varepsilon} = -k_2\rho$
3	recrystallisation	G, X, ρ	$\underleftrightarrow{\rho}$	$\rho > \rho_{cr}$	SANDSTROM and LAGNEBORG [8, 9]	$\frac{dX}{dt} = \frac{\nu\gamma}{D} m\tau G_i\rho_i$
4	grain refinement	D	$\underleftrightarrow{\rho}$	$\rho > \rho_{cr}$	SANDSTROM and LAGNEBORG [8, 9]	$\frac{dD}{dt} = -D\frac{dX}{dt}\ln N$
5	grain growth	D	$\underleftrightarrow{\rho}$	always	SANDSTROM and LAGNEBORG [8, 9]	$\frac{dD}{dt} = \frac{m\sigma_g}{D}$

All formulae used in the present volume distribution model are given in Tables 1 and 2. The following notation is used in these tables: b – Burgers vector, D – austenite grain size, d – dislocation cell size, G – volume distribution of dislocation density, l - dislocation mean free path, t – time, X – recrystallized volume fraction, Z – Zener-Hollomon parameter, ε – strain, $\dot{\varepsilon}$ – strain rate, γ – fraction of subgrain boundary which is migrating, μ – shear modulus, ρ – dislocation density, ρ_{cr} – critical dislocation density for nucleation, σ_g – grain boundary energy, τ – energy per unit length of dislocation.

Table 2. Equations in the volume distribution model

variable	Ref.	equation
cell size (free path)	ROBERTS and AHLBLOM [10]	$l = d = \dfrac{K_d}{Z^q}$
mobile fraction of boundary	PIETRZYK and KUZIAK [15]	$\gamma = [1 - \exp(-X)]\,(1 - X)\left(\dfrac{\rho}{\rho_{\mathrm{cr}}}\right)^{q_1}$
number of new grains per one old grain	SANDSTROM and LAGNEBORG [8, 9]	$N = 4\gamma\left(\dfrac{D}{d_s}\right)^2$
critical dislocation density	ROBERTS and AHLBLOM [10]	$\rho_{\mathrm{cr}} = \dfrac{8\sigma_g}{\tau l}$

3. FINITE ELEMENT MODEL

Rigid-plastic finite-element model is used to simulate metal flow and heat transfer during hot-forming processes. Details of this model are given in [16]. Briefly, the rigid-plastic approach is based on an extremum principle which states that for a plastically deforming body of volume V, under traction $\mathbf{f}$ prescribed on a part of the surface S and the velocity $\mathbf{v}$ prescribed on the remainder of S, the actual solution minimises the functional:

$$J = \int_V \sigma_i \dot{\varepsilon}_i dV - \int_S \mathbf{f}^T \mathbf{v} dS, \tag{3.1}$$

under the constraint $\dot{\varepsilon}_V = \dot{\varepsilon}_x + \dot{\varepsilon}_y + \dot{\varepsilon}_z = 0$. Penalty coefficient or Lagrange multiplier methods can be used to impose the incompressibility condition. It is convenient to use a Lagrange multiplier λ and a stationary value problem is then

obtained for the FEM analysis. The functional J becomes:

$$J = \int_V (\sigma_i \dot{\varepsilon}_i + \lambda \dot{\varepsilon}_V)\, dV - \int_S \mathbf{f}^T \mathbf{v} dS, \tag{3.2}$$

where σ_i – effective stress, $\dot{\varepsilon}$ – effective strain rate, $\dot{\varepsilon}_V$ – volumetric strain rate, $\mathbf{f}$ – vector of boundary tractions, $\mathbf{v}$ – vector of nodal velocities. Discretisation is performed in a typical finite element manner and the velocity components inside the element are given by interpolation: $\mathbf{v} = \{\nu_x, \nu_y, \nu_z\}^T = \mathbf{N}^T \mathbf{v}$, where ν_x, ν_y, ν_z – components of velocity, $\mathbf{N}$ – matrix of shape functions. The discretisation of the functional (3.2) follows the normal procedure. The strain rate field inside the element is related to the nodal velocities:

$$\dot{\boldsymbol{\varepsilon}} = \{\dot{\varepsilon}_x, \dot{\varepsilon}_y, \dot{\varepsilon}_z, \dot{\varepsilon}_{xy}, \dot{\varepsilon}_{yz}, \dot{\varepsilon}_{zx}\}^T = \mathbf{B}\mathbf{v}, \tag{3.3}$$

where: $\dot{\varepsilon}_x, \dot{\varepsilon}_y, \dot{\varepsilon}_z, \dot{\varepsilon}_{xy} \dot{\varepsilon}_{yz}, \dot{\varepsilon}_{zx}$ – components of the strain rate, $\mathbf{B}$ – matrix of derivatives of shape functions. Volumetric strain rate in Eq. (3.2) is calculated as $\dot{\varepsilon}_V = \mathbf{c}^T \dot{\boldsymbol{\varepsilon}}$, where $\mathbf{c}$ is such a vector that $\mathbf{c}^T \dot{\boldsymbol{\varepsilon}}$ yields the incompressibility condition. $\mathbf{c}^T$ equals {1,1,1,0,0,} for 3D, {1,1,0} for plane strain and {1,1,1,0} for axisymmetric problems. During discretisation, body with the volume V is divided into m elements connected by n nodes. The functional for the whole volume is a sum of the functionals for the elements. Introducing Eq. (3.3) into (3.2) gives:

$$J = \int_V \sigma_i \sqrt{\frac{2}{3} \mathbf{v}^T \hat{\mathbf{K}} \mathbf{v}}\, dV + \lambda \mathbf{v}^T \mathbf{q} - \mathbf{v}^T \hat{\mathbf{f}}, \tag{3.4}$$

where:

$$\hat{\mathbf{K}} = \mathbf{B}^T \mathbf{E} \mathbf{B} \qquad \mathbf{q} = \int_V \mathbf{B}^T \mathbf{c} dV, \qquad \hat{\mathbf{f}} = \int_S \mathbf{N}^T \mathbf{f} dS,$$

$\mathbf{E}$ – matrix in the Levy-Mises flow rule $\boldsymbol{\sigma} = \mathbf{E}\dot{\boldsymbol{\varepsilon}}$ [16], $\boldsymbol{\sigma}$ – vector containing stress components. Differentiation of Eq. (3.4) with respect to the nodal velocities and to the Lagrange multiplier yields a set of non-linear equations which, after Newton-Raphson linearization, takes the form:

$$\mathbf{p} = \mathbf{K} \begin{Bmatrix} \Delta \mathbf{v} \\ \lambda \end{Bmatrix}, \tag{3.5}$$

where

$$\mathbf{K} \begin{bmatrix} \dfrac{\partial^2 J}{\partial \mathbf{v}^T \partial \mathbf{v}} & \mathbf{q} \\ \mathbf{q} & 0 \end{bmatrix}, \qquad \mathbf{p} = \begin{Bmatrix} \dfrac{\partial J}{\partial \mathbf{v}^T} \\ \mathbf{q}^T \hat{\mathbf{v}} \end{Bmatrix},$$

$\hat{\mathbf{v}}$ – vector of nodal velocities calculated by previous iteration.

Solution of Eq. (3.5) yields the nodal velocity increments which, in the iterative procedure, allow the determination of the velocity field. The friction model with velocity-dependent friction forces described by arctan function, suggested by Li and Kobayashi and given also in [16], is used in the solutions.

The solution is coupled with the thermal model. Temperatures are calculated accounting for heat conduction in the material, heat generation due to the plastic work and friction, heat losses due to transfer to the surrounding medium. The approach is based on the equation:

$$\nabla(k\nabla T) + Q = c_p \rho \frac{\partial T}{\partial t}. \tag{3.6}$$

The equation (3.6) is used in modelling of the non-stationary processes like forging. Such processes as rolling develop stationary temperature fields in the co-ordinate system connected with the tool and are simulated by the general convection-diffusion equation:

$$\nabla(k\nabla T) + Q = c_p \rho \mathbf{v}^T \nabla T, \tag{3.7}$$

where k – conductivity, ρ – density, c_p – specific heat, T – temperature, Q – heat generated due to plastic work, t – time. Solution of Eq. (3.7) for steady state problems with convection with the relevant boundary conditions yields a set of linear equations

$$\mathbf{Ht} = \mathbf{p},$$

with $\mathbf{t}$ being the vector of nodal temperatures and matrices $\mathbf{H}$ and $\mathbf{p}$ given by

$$H_{ij} = \int_V \left[k \left(\frac{\partial N_i}{\partial x}\frac{\partial N_j}{\partial x} + \frac{\partial N_i}{\partial y}\frac{\partial N_i}{\partial y} \right) - \nu_{xi}\frac{\partial N_j}{\partial x} - \nu_{yi}\frac{\partial N_j}{\partial y} \right] dV + \int \alpha N_i N_j dS,$$

$$p_i = \int_V N_i Q dV + \int_S N_i (q + T_0) dS,$$

where q – heat generated due to friction, α – heat transfer coefficient, T_0 – ambient temperature or tool temperature, N – shape functions.

The non-steady state solution of Eq. (3.6) using Galerkin approach gives a set of equations:

$$\hat{\mathbf{H}}\mathbf{t} = \hat{\mathbf{p}}$$

where

$$\hat{\mathbf{H}} = \left(2\mathbf{H} + \frac{3}{\Delta t}\mathbf{C} \right), \quad \hat{\mathbf{p}} = \left(-\mathbf{H} + \frac{3}{\Delta t}\mathbf{C} \right) \mathbf{t}_0 - 3\mathbf{p}, \quad C_{ij} = \int_V N_i c_p \rho N_j dV,$$

$\mathbf{t}_0$ – vector of nodal temperatures at the beginning of time interval Δt.

The finite-element model described above is connected with the internal variable approach, which is used as a constitutive law in this model. Exactly, the yield stress connecting stress components with the strain rate components in the Levy-Mises flow rule is calculated from Eq. (2.7), accounting for the current distribution of dislocation densities in each element in the finite-element mesh. On the other hand, current local values of strain rates, temperatures and strain increments predicted by the finite element model in one time increment are used in the internal variable approach for calculations of the changes of dislocation density distribution.

4. Results and analysis

Developed thermal-mechanical-microstructural model has been successfully applied to the modelling of hot forming of steels [17] in constant temperatures and strain rates. Experiments [18] confirmed proper model's performance in the transient state, as well. Figure 2 shows typical results of simulation of compression test for carbon-manganese steels with the strain rate changing rapidly at the strain of 0.18 [18]. It is seen in this figure that the transient behaviour is negligible in the case of increasing strain rate. Response of the system reaches a level determined by the equation of state for the new conditions almost immediately. In the case of a decreasing strain rate, the delay of the response is larger and this response reaches the level below that determined by the equation of state for the new conditions. Figure 3 shows the results of measurements [19] and calculations of compression stress during the test performed in the temperature decreasing continuously from 1150 °C to 950 °C. Recapitulating the results of all measurements and calculations [18, 19], it can be concluded that the model predicts properly the yield stress during transient hot deformation of steels.

Modelling of transient hot deformation of aluminium alloys presents more difficulties. The experimental results for transient compression tests published in the scientific literature [20, 21] show differences in the behaviour of high purity (HP) and commercial purity (CP) alloys containing 1% of magnesium. Modelling of the yield stress for these alloys is based on Eq. (2.8) with additional terms accounting for the influence of the dislocation slip σ_f and for the influence of subgrain boundaries:

$$\sigma = \sigma_f + \alpha_1 M_T \alpha \mu b \sqrt{\rho} + \frac{\alpha_2 M_T \mu}{\delta}, \tag{4.1}$$

where δ – distance between subgrain boundaries, α_1, α_2 – constants.

Since the third term in Eq. (4.1) is small, explanation of the transient behaviour of aluminium alloys is connected with the two remaining terms. Relation

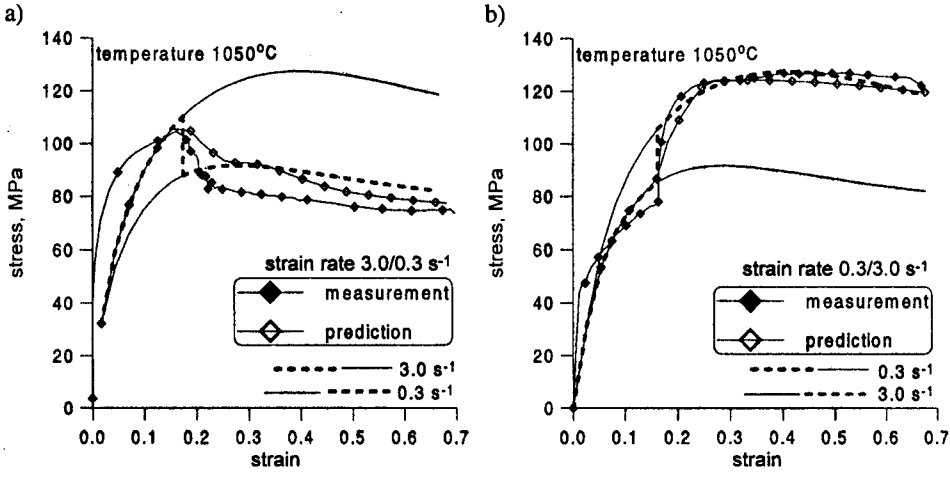

FIG. 2. Results of calculations and measurements of compression stress for a steel specimen deformed under the strain rate changing rapidly, at the strain of 0.18; a) increase of the strain rate, b) decrease of the strain rate.

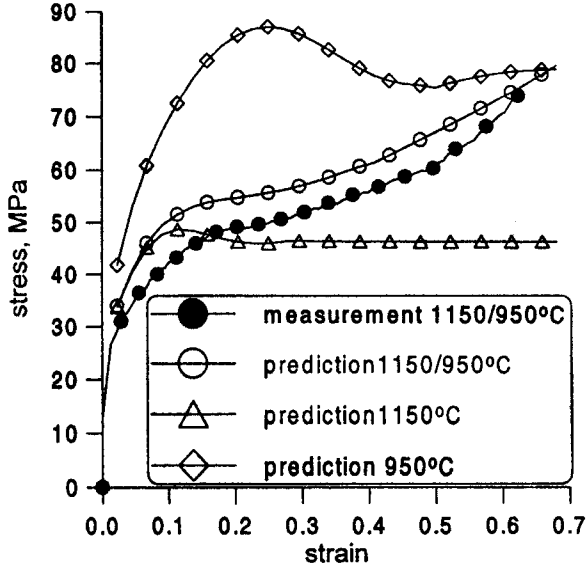

FIG. 3. Results of calculations and measurements of compression stress for steel sample deformed in the temperatures changing from 1150 °C to 950 °C.

between the strain rate and the development of the dislocation substructure is given by the Orowan's equation:

$$\dot{\varepsilon} = \frac{\rho b \nu}{M_T}, \tag{4.2}$$

where ν – average rate of dislocations.

In the case of change of the strain rate, the dislocation density does not change right away. With some delay it tends to the new value proportional to σ^2. Authors of [20] suggest that compensatory influence of dislocation σ_f is responsible for lack of transient state in some cases. Rate of dislocations connected with climb ν is proportional to σ^3, what means that decrease of stress gives instantaneous decrease in ν. On the other hand, recovery increases this rate and yields an increase of the rate of deformation. In alloys with higher Mg contents, proportionality $\nu \sim \sigma$ takes place, what means that rate ν changes immediately and remains constant, yielding a decrease of the rate of deformation in time.

The analysis presented above shows that the constants in the internal variable model given by Eq. (4.1) cannot be determined from the tests carried out under constant conditions. Therefore, the experimental results for variable strain rates presented in [21] were used in this paper to test the model. The resulting comparison of the measured [20] and calculated compression stress during the test with the constant strain rate and the strain rate changing continuously from 25 s^{-1} to 2.5 s^{-1} are shown in Fig. 4. It is seen in this figure that the model describes transient behaviour of aluminium alloy quite well.

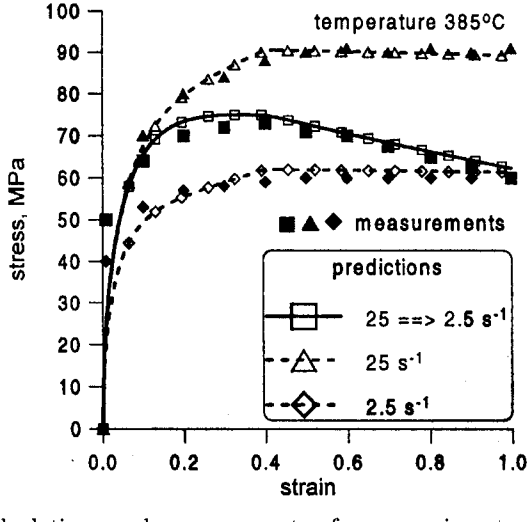

FIG. 4. Results of calculations and measurements of compression stress for aluminium alloy sample deformed with the strain rate changing continuously from 25 s^{-1} to 2.5 s^{-1}.

5. Conclusions

It is shown in the paper that modelling of the transient behaviour of metals during hot deformation cannot be based on conventional models with the external variables used as independent variables. Good results of modelling have been obtained when an internal variable representing the energy accumulated in the dislocation substructure is used. In general, the metals exhibit two kinds of transient behaviour. When an interaction between dislocations is a dominant factor contributing to the stress, the metal shows delay of the response during transient deformation. On the other hand, in some cases when a compensatory influence of dislocation slip (σ_f is prevailing), the lack of transient state may be observed.

Acknowledgements

Financial assistance of KBN (grant. no. 7 T08B 042 14) is gratefully acknowledged.

References

1. C.M. Sellars, *Modelling – an interdisciplinary activity*, Proc. Symp. Mathematical Modelling of Hot Rolling of Steel [Ed.] S. Yue, Hamilton 1990, 1–18.
2. P.D. Hodgson, D. McFarlane and R.K. Gibbs, *The mathematical modelling of hot rolling: accuracy vs. utility*, Proc. Conf. Modelling of Metal Rolling Processes, London 1993, 2–15.
3. Q. Zhu and C.M. Sellars, *Recrystallisation behaviour in tension/tension and tension/compression hot deformation of Al.-2Mg*, Proc. Conf., Thermo-Mechanical Processing in Theory, Modelling and Practice, Eds., B. Hutchinson, M. Andersson, G. Engberg, B. Karlsson, T. Siwecki, Sztokholm 1996, 193–200.
4. A. Korbel, *Perspectives of the control of mechanical performance of metals during forming operations*, Proc. Conf. Metal Forming'92 [Eds.] M. Pietrzyk, J. Kusiak, J. Mat. Proc. Technol., **34**, 41–50, 1992.
5. Y. Estrin, *Dislocation density related constitutive modelling, unified constitutive laws of plastic deformation* [Eds.] A.S. Krausz, K. Krausz, Academic Press, 1996.
6. H. Mecking, U.F. Kocks, *Kinetics of flow and strain-hardening*, Acta Metall., **29**, 1865–1875, 1981.
7. Y. Estrin, H. Mecking, *A unified phenomenological description of work hardening and creep based on one-parameter models*, Acta Metall., **32**, 57–70, 1984.
8. R. Sandstrom, R. Lagneborg, *A model for hot working occurring by recrystallisation*, Acta Metall., **23**, 387–398, 1975.

9. R. SANDSTROM, R. LAGNEBORG, *A model for static recrystallisation after hot deformation*, Acta Metall., **23**, 481–488, 1975.

10. W. ROBERTS, B. AHLBLOM, *A mucleation criterion for dynamic recrystallisation during hot working*, Acta Metall. **26**, 801–813, 1978.

11. H.J. MCQUEEN, *Controversies in the theory of dynamic recrystallisation*, Mat. Sci. Forum, 113–115, 429–434, 1993.

12. S. WIERZBINSKI and A. KORBEL, *Some aspects of dynamic restoration processes in Cu-10Ni alloy*, High Temp. Metar. Proc., **12**, 105–116, 1993.

13. C.H.J. DAVIES, *Dynamics of the evolution of dislocation populations*, Scr. Metall. Mater., **30**, 349–353, 1994.

14. M. PIETRZYK, *Numerical aspects of the simulation of hot metal forming using internal variable method*, Metall. Foundry Eng., **20**, 429–439, 1994.

15. M. PIETRZYK, R. KUZIAK, *Application of the internal variable approach to the simulation of microstructural phenomena in hot forming of eutectoid steel*, Proc. Conf. EUROMAT'95, Padua 1995, 239–244.

16. M. PIETRZYK, J.G. LENARD, *Thermal-mechanical modelling of the flat rolling processes*, Springer-Verlag, Berlin 1991.

17. M. PIETRZYK, C. ROUCOULES, P.D. HODGSON, *Dislocation model for work hardening and recrystallisation applied to the finite-element simulation of hot forming*, Proc. Conf. NUMIFORM'95, [Eds.] S.-F. Shen, P.R. Dawson, Ithaca 1995, 315–320.

18. M. PIETRZYK and R. KUZIAK, *Validation of the history dependent flow stress model for hot forming of metals*, Proc. Conf. COMPLAS 5 [Eds.] D.R.J. Owen, E. Onate, E. Hinton, Barcelona 1997, 1363–1368.

19. R. KUZIAK, private information, Gliwice 1998.

20. Q. ZHU, H.R. SHERCLIFF, C.M. SELLARS, *Modelling hot deformation behaviour based on evolution of dislocation substructures*, Proc. Conf. THERMEC'97, [Eds.] T. Chandra, T. Sakai, Wollongong 1997, 2039–2045.

21. C.M. SELLARS, Q. ZHU, *Microstructural evolution during hot deformation of aluminium-magnesium alloys*, Proc. Symp. Hot Deformation of Aluminium, Rosemont 1998 (in press).

Received January 15, 1999.